
Vesoljska tehnika - Priročnik za toplotno zasnovno - 12. del: Žaluzije

Space Engineering - Thermal design handbook - Part 12: Louvers

Raumfahrttechnik - Handbuch für thermisches Design - Teil 12: Luftschlitze

Ingénierie spatiale - Manuel de conception thermique - Partie 12: Persiennes

Ta slovenski standard je istoveten z: FprCEN/CLC/TR 17603-31-12

[kSIST-TP FprCEN/CLC/TR 17603-31-12:2021](https://standards.iteh.ai/catalog/standards/sist/26a39d95-b01c-4490-90ce-f8a3adfc41e/ksist-tp-fprcen-clc-tr-17603-31-12-2021)

<https://standards.iteh.ai/catalog/standards/sist/26a39d95-b01c-4490-90ce-f8a3adfc41e/ksist-tp-fprcen-clc-tr-17603-31-12-2021>

ICS:

49.140 Vesoljski sistemi in operacije Space systems and operations

kSIST-TP FprCEN/CLC/TR 17603-31-12:2021 en,fr,de

iTeh STANDARD PREVIEW
(standards.iteh.ai)

[kSIST-TP FprCEN/CLC/TR 17603-31-12:2021](https://standards.iteh.ai/catalog/standards/sist/26a39d95-b01c-4490-90ce-f8a3adfc41e/ksist-tp-fprcen-clc-tr-17603-31-12-2021)
<https://standards.iteh.ai/catalog/standards/sist/26a39d95-b01c-4490-90ce-f8a3adfc41e/ksist-tp-fprcen-clc-tr-17603-31-12-2021>

TECHNICAL REPORT
RAPPORT TECHNIQUE
TECHNISCHER BERICHT

FINAL DRAFT
FprCEN/CLC/TR 17603-31-12

March 2021

ICS 49.140

English version

Space Engineering - Thermal design handbook - Part 12: Louvers

Ingénierie spatiale - Manuel de conception thermique -
Partie 12: Persiennes

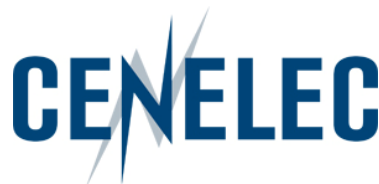
Raumfahrttechnik - Handbuch für thermisches Design -
Teil 12: Luftschlitze

This draft Technical Report is submitted to CEN members for Vote. It has been drawn up by the Technical Committee CEN/CLC/JTC 5.

CEN and CENELEC members are the national standards bodies and national electrotechnical committees of Austria, Belgium, Bulgaria, Croatia, Cyprus, Czech Republic, Denmark, Estonia, Finland, France, Germany, Greece, Hungary, Iceland, Ireland, Italy, Latvia, Lithuania, Luxembourg, Malta, Netherlands, Norway, Poland, Portugal, Republic of North Macedonia, Romania, Serbia, Slovakia, Slovenia, Spain, Sweden, Switzerland, Turkey and United Kingdom.

Recipients of this draft are invited to submit, with their comments, notification of any relevant patent rights of which they are aware and to provide supporting documentation.

Warning : This document is not a Technical Report. It is distributed for review and comments. It is subject to change without notice and shall not be referred to as a Technical Report.



CEN-CENELEC Management Centre:
Rue de la Science 23, B-1040 Brussels

Table of contents

European Foreword	7
1 Scope	8
2 References	9
3 Terms, definitions and symbols	10
3.1 Terms and definitions	10
3.2 Symbols.....	10
4 General introduction	15
5 Components of a louver	16
5.1 Blades	16
5.2 Actuators	18
5.2.1 Bimetals	18
5.2.2 Bellows	24
5.2.3 Bourdons	35
5.3 Sensors	37
5.3.1 Sensor location	37
5.3.2 Coupling options	38
5.4 Structural elements.....	38
5.4.1 Actuator housing	38
5.4.2 Frames.....	38
6 Ideal louvers	40
6.1 Sun-light operation.....	40
6.1.1 Introduction	40
6.1.2 Heat rejection capability	40
6.1.3 Effective absorptance.....	43
6.1.4 Effective emittance.....	46
6.2 Shadow operation.....	52
6.2.1 Introduction	52
6.2.2 Radiosity and temperature field of the blades.....	53
6.2.3 Heat transfer through the louver	55

7 Existing systems	66
7.1 Summary table	66
7.2 Ats louvers.....	76
7.2.1 Introduction	76
7.2.2 Analytical calculations	76
7.2.3 Tests	80
7.3 Nimbus louvers.....	83
7.3.1 Introduction	83
7.3.2 Louvers of the sensory subsystem	83
7.3.3 Louver of the control subsystem.....	84
7.3.4 Flight performance	86
7.4 Snias louvers	87
7.4.1 Introduction	87
7.4.2 Analytical calculations	88
7.4.3 Tests	95
7.4.4 The Bourdon tube used as an actuator in the SNIAS Louver system	98
Bibliography.....	104

iTeh STANDARD PREVIEW

(standards.iteh.ai)

Figures

Figure 5-1: Relative linear thermal expansion vs. temperature in the case of Invar. $T_0 = 273$ K. From THE MOND NICKEL CO [35].....	19
Figure 5-2: Relative linear thermal expansion vs. temperature in the case of brasses. $T_0 = 273$ K. After Baldwin (1961) [3].....	20
Figure 5-3: Relative linear thermal expansion vs. temperature in the case of austenitic steels. $T_0 = 273$ K. After Zapffe (1961) [39].	20
Figure 5-4: Relative linear thermal expansion vs. temperature in the case of Nimonic alloys. $T_0 = 273$ K. After WIGGIN & Co. (1967) [38].....	21
Figure 5-5: Relative linear thermal expansion vs. temperature for different alloys. $T_0 = 273$ K. After Baldwin (1961) [3], Zapffe (1961) [39], WIGGIN Co. (1967) [38].....	21
Figure 5-6: Difference of temperature, ΔT , vs. angle of rotation of the free end, θ , for several values of the sensitivity, X . After Martin & Yarworth (1961) [21], KAMMERER (1971) [16].	22
Figure 5-7: Sensitivity vs. ratio L/t , for different values of K_c . After Martin & Yarworth (1961) [21], KAMMERER (1971) [16].	23
Figure 5-8: Dimensionless ratio $M/K_c F_c \Delta T L^3$ vs. L/t , for several values of w/t . After Martin & Yarworth (1961) [21], KAMMERER (1971) [16].	24
Figure 5-9: Values of α and β vs. ratio a/b for different cross sections of the Bourdon tube. After Trylinski (1971) [37].	36
Figure 5-10: Ratio F/F_0 vs. Bourdon initial coiling angle, ψ_0 . Calculated by the compiler.....	37

FprCEN/CLC/TR 17603-31-12:2021 (E)

Figure 6-1: Geometry of the blade-baseplate system	40
Figure 6-2: Heat rejection capability, q , vs. blade angle, θ , for several values of the sun angle, ϕ . From FAIRCHILD HILLER (1972) [10].	42
Figure 6-3: Heat rejection capability, q , vs. blade angle, θ , for several values of the sun angle, ϕ . From Parmer & Stipandic (1968) [27].	43
Figure 6-4: Effective absorptance, α_{eff} , vs. blade angle, θ , for several values of the sun angle, ϕ . After FAIRCHILD HILLER (1972) [10].	45
Figure 6-5: Effective absorptance, α_{eff} , vs. blade angle, θ , for several values of the sun angle, ϕ . After Parmer & Stipandic (1968) [27].	46
Figure 6-6: Effective emittance, ε_{eff} , vs. blade angle, θ . After FAIRCHILD HILLER (1972) [10].	48
Figure 6-7: Effective emittance, ε_{eff} , vs. blade angle, θ . After Parmer & Stipandic (1968) [27].	49
Figure 6-8: Effective emittance, ε_{eff} , vs. blade angle, θ , for several values of the baseplate emittance, ε_{BP} . ε_{eff} has been numerically calculated by using the following expression. $\varepsilon_{eff} = \frac{\varepsilon_{BP}}{1 - \varepsilon_{BP}} \int_0^1 (1 - B^*) d\beta$	50
Figure 6-9: Effective emittance, ε_{eff} , vs. blade angle, θ , for several values of the blades emittance, ε_B . ε_{eff} has been numerically calculated by using the following expression. $\varepsilon_{eff} = \frac{\varepsilon_{BP}}{1 - \varepsilon_{BP}} \int_0^1 (1 - B^*) d\beta$	51
Figure 6-10: Effective emittance, ε_{eff} , vs. blade angle, θ , for several b/L values. ε_{eff} has been numerically calculated by using the following expression. $\varepsilon_{eff} = \frac{\varepsilon_{BP}}{1 - \varepsilon_{BP}} \int_0^1 (1 - B^*) d\beta$	52
Figure 6-11: Schematic diagram of a louver for shadow operation.	53
Figure 6-12: Schematic diagram of the louver array showing the coordinates and the significant geometrical characteristics.	54
Figure 6-13: Dimensionless radiosity, B^* , of the blades for several values of the blade angle, θ . From Plamondon (1964) [28].	55
Figure 6-14: Dimensionless temperature, T^* , of the blades for several values of the blade angle, θ . From Plamondon (1964) [28].	55
Figure 6-15: Function $f(\theta)$ vs. blade angle θ . After Parmer & Buskirk (1967)a [25].	57
Figure 6-16: Net heat transfer through the louver, q , vs. baseplate temperature, T_{BP} , for several values of the blade angle, θ . $\varepsilon_B = 0,05$, $\varepsilon_{BP} = \varepsilon_l = 0.87$. Calculated by the compiler.	58
Figure 6-17: Net heat transfer through the louver, q , vs. baseplate temperature, T_{BP} , for several values of the blade angle, θ . $\varepsilon_B = 0,05$, $\varepsilon_{BP} = \varepsilon_l = 0,87$. Calculated by the compiler.	59
Figure 6-18: Net heat transfer through the louver, q , vs. baseplate temperature, T_{BP} , for several values of the blade angle, θ . $\varepsilon_B = 0,05$, $\varepsilon_{BP} = \varepsilon_l = 0,87$. Calculated by the compiler.	60

Figure 6-19: Net heat transfer through the louver, q , vs. baseplate temperature, T_{BP} , for several values of the blade angle, θ . $\varepsilon_B = 0,05$, $\varepsilon_{BP} = \varepsilon_l = 0,87$. Calculated by the compiler.....	61
Figure 6-20: Net heat transfer through the louver, q , vs. baseplate temperature, T_{BP} , for several values of the blade angle, θ . $\varepsilon_B = 0,05$, $\varepsilon_{BP} = \varepsilon_l = 0,87$. Calculated by the compiler.....	62
Figure 6-21: Net heat transfer through the louver, q , vs. baseplate temperature, T_{BP} , for several values of the blade angle, θ . $\varepsilon_B = 0,05$, $\varepsilon_{BP} = \varepsilon_l = 0,87$. Calculated by the compiler.....	63
Figure 6-22: Net heat transfer through the louver, q , vs. baseplate temperature, T_{BP} , for several values of the blade angle, θ . $\varepsilon_B = 0,05$, $\varepsilon_{BP} = \varepsilon_l = 0,87$. Calculated by the compiler.....	64
Figure 6-23: Net heat transfer through the louver, q , vs. baseplate temperature, T_{BP} , for several values of the blade angle, θ . $\varepsilon_B = 0,05$, $\varepsilon_{BP} = \varepsilon_l = 0,87$. Calculated by the compiler.....	65
Figure 7-1: Effective emittance, ε_{eff} , based on area of the large unit, vs. blade angle, θ , for ATS spacecraft. From Michalek, Stipandic & Coyle (1972) [24].....	78
Figure 7-2: Effective absorptance, α_{eff} , vs. blade angle, θ , for several values of the sun angle, ϕ , for ATS spacecraft. From Michalek, Stipandic & Coyle (1972) [24].	79
Figure 7-3: Heat rejection capability, q , vs. blade angle, θ , for several values of the sun angle, ϕ , for ATS spacecraft. From Michalek, Stipandic & Coyle (1972) [24].	80
Figure 7-4: Effective absorptance, α_{eff} , vs. sun angle, ϕ , for several values of the blade angle, θ , for ATS spacecraft. From Michalek, Stipandic & Coyle (1972) [24].	81
Figure 7-5: Heat rejection capability, q , vs. sun angle, ϕ , for ATS spacecraft. From Michalek, Stipandic & Coyle (1972) [24].	82
Figure 7-6: Effective emittance vs. blade angle, θ , and baseplate temperature, T_{BP} , for sensory subsystem of NIMBUS spacecraft. From London (1967) [20].....	84
Figure 7-7: Schematic blade geometry for diffuse body radiation analysis. Louvers of the control subsystem. NIMBUS spacecraft. From London (1967) [20].	85
Figure 7-8: Effective emittance, ε_{eff} , vs. blade angle, θ , for the control subsystem of NIMBUS spacecraft. From London (1967) [20].....	85
Figure 7-9: Effective emittance, ε_{eff} , vs. baseplate temperature, T_{BP} , for the control subsystem of NIMBUS spacecraft. From London (1967) [20].	86
Figure 7-10: Comparison of NIMBUS 1 and 2 control subsystem panel temperatures, T_p , vs. orbital position. From London (1967) [20].	86
Figure 7-11: Overall dimensions of SNIAS louver. Not to scale.	87
Figure 7-12: Effective emittance, ε_{eff} , vs. blade angle, θ , for the SNIAS louver system. From Redor (1972) [29].....	89
Figure 7-13: Effective absorptance, α_{eff} , vs. blade angle, θ , for several values of the sun angle, ϕ . SNIAS louver system. From Redor (1972) [29].	91
Figure 7-14: Heat rejection capability, q , vs. blade angle, θ , for several values of the sun angle, ϕ . SNIAS louver system. From Redor (1972) [29].....	93
Figure 7-15: Maximum blade temperature, T_B , vs. blade angle, θ , for several values of the sun angle, ϕ . SNIAS louver system. From Redor (1972) [29].....	95

FprCEN/CLC/TR 17603-31-12:2021 (E)

Figure 7-16: Effective emittance, ϵ_{eff} , vs. blade angle, θ , for the louver system of SNIAS. Solid line: From Redor (1972) [29]. Dashed line: From Croiset & Leroy (1973) [8].....	96
Figure 7-17: Heat rejection capability, q , vs. blade angle, θ , for several values of the sun angle, ϕ . SNIAS louver system. Solid line: From Redor (1972) [29]. Dashed line: From Croiset & Leroy (1973) [8].....	97
Figure 7-18: Temperature-pressure characteristic of the Bourdon spiral. From Reusser et al. (1973) [30].....	100
Figure 7-19: Performance of a Bourdon actuating a single blade. After Reusser et al. (1973) [30].....	101
Figure 7-20: Ratios $(T_{BP}-T)/(T_{BP}-T_{OL})$ and Q/Q_0 vs. time, τ . After Reusser et al. (1973) [30].....	103

Tables

Table 5-1: Blade Characteristics of Existing Louver Assemblies R: Rectangular, T: Trapezoidal	16
Table 5-2: Materials Used	19
Table 5-3: Typical Alloy Used in Bellows D: Deposited, F: Formed, W: Welded	25
Table 5-4: Typical Nonmetallic Materials Used in Bellows	27
Table 5-5: Typical Fluids Used in Bellows	28
Table 5-6: Bellows Convolutions and Relevant Characteristics	28
Table 5-7: Spring Rate for Several Bellows	30
Table 5-8: Frequency of Bellows Vibration	31
Table 5-9: Characteristics of Convolved Bellows	32
Table 7-1: Assumed Values of the Optical Properties of the Surfaces for the First Computer program	77
Table 7-2: Assumed Values of the Optical Properties of the Surfaces for the Second Computer program	77
Table 7-3: Ideal Optical Properties of the NIMBUS Louvers Surfaces	83
Table 7-4: Optical Characteristics of the Surfaces of SNIAS Louver.....	87
Table 7-5: Effective Absorptance α_{eff} , for Several Values of Sun Angle, ϕ , and Blade Angle, θ	90
Table 7-6: Heat Rejection Capability, q , for Several Values of Sun Angle, ϕ , and Blade Angle, θ	92
Table 7-7: Maximum Blade Temperature, T_B , for Several Values of Sun Angle, ϕ , and Blade Angle, θ	94
Table 7-8: Several Characteristics of the Bourdon Spiral.....	98
Table 7-9: Several Parameters of the Bourdon Spiral.....	99

European Foreword

This document (FprCEN/CLC/TR 17603-31-12:2021) has been prepared by Technical Committee CEN/CLC/JTC 5 "Space", the secretariat of which is held by DIN.

This document is currently submitted to the Vote on TR.

It is highlighted that this technical report does not contain any requirement but only collection of data or descriptions and guidelines about how to organize and perform the work in support of EN 16603-31.

This Technical report (FprCEN/CLC/TR 17603-31-12:2021) originates from ECSS-E-HB-31-01 Part 12A.

Attention is drawn to the possibility that some of the elements of this document may be the subject of patent rights. CEN [and/or CENELEC] shall not be held responsible for identifying any or all such patent rights.

This document has been prepared under a mandate given to CEN by the European Commission and the European Free Trade Association.

This document has been developed to cover specifically space systems and has therefore precedence over any TR covering the same scope but with a wider domain of applicability (e.g.: aerospace).

This document is currently submitted to the CEN CONSULTATION.

ITih STANDARD PREVIEW
(standards.iteh.ai)
kSIST-TP FprCEN/CLC/TR 17603-31-12:2021
<https://standards.iteh.ai/catalog/standards/sist/2023/09/10/cen-4490-90ce-f8a3adfc41e/ksist-tp-fprcen-clc-tr-17603-31-12-2021>

1

Scope

Thermal louvers are thermal control surfaces whose radiation characteristics can be varied in order to maintain the correct operating temperature of a component subject to cyclical changes in the amount of heat that it absorbs or generates.

The design and construction of louvers for space systems are described in this Part 12 and a clause is also dedicated to providing details on existing systems.

The Thermal design handbook is published in 16 Parts

TR 17603-31-01	Thermal design handbook – Part 1: View factors
TR 17603-31-02	Thermal design handbook – Part 2: Holes, Grooves and Cavities
TR 17603-31-03	Thermal design handbook – Part 3: Spacecraft Surface Temperature
TR 17603-31-04	Thermal design handbook – Part 4: Conductive Heat Transfer
TR 17603-31-05	Thermal design handbook – Part 5: Structural Materials: Metallic and Composite
TR 17603-31-06	Thermal design handbook – Part 6: Thermal Control Surfaces
TR 17603-31-07	Thermal design handbook – Part 7: Insulations
TR 17603-31-08	Thermal design handbook – Part 8: Heat Pipes
TR 17603-31-09	Thermal design handbook – Part 9: Radiators
TR 17603-31-10	Thermal design handbook – Part 10: Phase – Change Capacitors
TR 17603-31-11	Thermal design handbook – Part 11: Electrical Heating
TR 17603-31-12	Thermal design handbook – Part 12: Louvers
TR 17603-31-13	Thermal design handbook – Part 13: Fluid Loops
TR 17603-31-14	Thermal design handbook – Part 14: Cryogenic Cooling
TR 17603-31-15	Thermal design handbook – Part 15: Existing Satellites
TR 17603-31-16	Thermal design handbook – Part 16: Thermal Protection System

2 References

EN Reference	Reference in text	Title
EN 16601-00-01	ECSS-S-ST-00-01	ECSS System - Glossary of terms

All other references made to publications in this Part are listed, alphabetically, in the **Bibliography**.

iTeh STANDARD PREVIEW (standards.iteh.ai)

[kSIST-TP FprCEN/CLC/TR 17603-31-12:2021
https://standards.iteh.ai/catalog/standards/sist/26a39d95-b01c-4490-90ce-f8a3adfc41e/ksist-tp-fprcen-clc-tr-17603-31-12-2021](https://standards.iteh.ai/catalog/standards/sist/26a39d95-b01c-4490-90ce-f8a3adfc41e/ksist-tp-fprcen-clc-tr-17603-31-12-2021)

Terms, definitions and symbols

3.1 Terms and definitions

For the purpose of this Standard, the terms and definitions given in ECSS-S-ST-00-01 apply.

3.2 Symbols

A	Clause 5: bellows effective area, [m ²]
	Clause 7: contact surface (bourdon sensing element), [m ²]
B	radiosity, [W.m ⁻²]
B*	dimensionless radiosity, $B^* = B/\sigma T^4$
D _i	bellows innermost diameter, [m]
D _o	bellows outermost diameter, [m]
E	modulus of elasticity, [N.m ⁻²]
F	flexibility, [m.Pa ⁻¹]
F _c	coil force constant, [N.m ⁻² .Angular degrees ⁻¹]
H	energy flux impinging on the unit area, [W.m ⁻²]
J	heat flux to the skin arriving from outside, [W.m ⁻²]
K	bellows spring rate, [N.m ⁻¹]
K _c	coil deflection constant, [angular degrees, K ⁻¹]
L	Clause 5: coil active length, [m]
	Clause 5: length of all convolutions in bellows, [m]
	Clause 6: louver blade spacing, [m]

FprCEN/CLC/TR 17603-31-12:2021 (E)

L_c	length of a single convolution in bellows measured along the surface, [m]
M	torsional moment of a coil, [N.m]
P	fluid pressure, [Pa]
P_t	proportionality limit pressure in a bourdon, [Pa]
Q	heat transfer to the fluid within the bourdon, [J]
Q_0	heat transfer to the fluid within the bourdon after an infinitely large time, [J]
$R(\theta)$	equivalent thermal resistance of the louver system, it is a function of the optical properties of blades, and inner skin surface, but for a given system R depends only on the blade angle
R_0	coiling radius of a bourdon, [m]
R_m	mean radius of the bellows, [m]
S	heat flux from the space to the skin, [$W \cdot m^{-2}$]
S_0	solar constant, $S_0 = 1353 \text{ W} \cdot m^{-2}$
T	temperature, [K]
T_c	bourdon filling fluid temperature, [K]
T_0	reference temperature, [K]
ΔT	temperature differential, [K], $\Delta T = T - T_0$
T_{0L}	starting fluid temperature, [K]
T_s	skin temperature, [K]
T^*	local dimensionless temperature, $T^* = T^4 / T_{BP}^4$
V	inside volume of bellows, [m^3]
X	sensitivity of a bimetal, [angular degrees, K^{-1}]
a	semi-major axis of the bourdon tube cross section, [m]
b	Clause 5: semi-minor axis of the bourdon tube section, [m] Clause 6: louver blade width, [m]

STANDARD PREVIEW
(standards.iteh.ai)

kSIST-TP FprCEN/CLC/TR 17603-31-12:2021
temperature, [K]
<https://standards.iteh.ai/catalog/standards/sist/26a59d95-b01c-4490-90ce-f8a3adfc41e/ksist-tp-fprcen-clc-tr-17603-31-12-2021>

FprCEN/CLC/TR 17603-31-12:2021 (E)

c	Clause 5: numerical coefficient given in Table 5-7 under additional data Clause 7: fluid specific heat, [J.kg ⁻¹ .K ⁻¹]
f(θ)	defined as $f(\theta) = 1 - [1/R(\theta)]$
f_{n=1}	fundamental natural frequency, [s ⁻¹]
h	total thermal conductance of a bourdon (sensing element plus fluid), [W.m ⁻² .K ⁻¹]
l	length of a given metallic strip when the temperature is <i>T</i> [m] live length of the bellows, [m]
l₀	length of a given metallic strip when the temperature is <i>T</i> ₀ , [m]
m_a	mass of bellows active convolutions, [kg]
m_c	mass of one convolution, [kg]
m_{fa}	mass of fluid trapped in active length at rest, [kg] $m_{fa} = \rho L[0,262(D_o^2 + D_o D_i) - 0,524 D_i^2]$
m_l	mass of liquid within the bellows, [kg]. $m_l = \rho A l$
m₁	mass on bellows free end, [kg]
m₂	bellows mass, [kg]
q	louver heat rejection capability, [W.m ⁻²]
q_{shadow}	heat rejection capability for zero solar input, [W.m ⁻²]
t	thickness of the strip of the coil, [m] wall thickness for bellows or bourdon tube, [m]
w	width of the strip of the coil, [m]
x	coordinate along the louver baseplate, [m]
y,z	Coordinates along the outer and inner faces of the blade, [m]
Φ	sun angle, [angular degrees]
α	absorptance

	numerical coefficient which appears in the expression of bourdon flexibility
α_s	solar absorptance
α_λ	spectral absorptance
β	Clause 5: linear thermal expansion coefficient, [K ⁻¹] Clause 5: numerical coefficient which appears in that expression of bourdon flexibility Clause 6: Dimensionless coordinate along the louver baseplate, $\beta = x/L$
β_H	linear thermal expansion coefficient of the high expansibility component of a bimetal, [K ⁻¹]
β_L	linear thermal expansion coefficient of the low expansibility component of a bimetal, [K ⁻¹]
ε	hemispherical total emittance
ε_i	emittance of the skin inner surface
ε_s	emittance of the skin outer surface
η, ζ	dimensionless coordinates, $\eta = y/L$, $\zeta = z/L$
θ	Clause 5: angular deflection of a coil, [angular degrees] Clause 6: louver blade angle, [angular degrees]
ν	poisson's ratio
ρ	Clauses 5 and 7: fluid density, [kg.m ⁻³] Clause 6: reflectance
ρ_λ	spectral reflectance
ρ^s	specular reflectance
ψ_0	initial coiling angle in a bourdon, also called mechanical preload angle, [angular degrees]
σ	Stefan-Boltzmann constant, $\sigma = 5,6697 \times 10^{-8}$ W.m ⁻² .K ⁻⁴
τ	time, [s]

iTech STANDARD PREVIEW
(standards.iteh.ai)

kSIST-TP FprCEN/CLC/TR 17603-31-12:2021
<https://standards.iteh.ai/catalog/standards/sist/26a39d95-b01c-4490-90ce-f8a3adfc41e/ksist-tp-fprcen-clc-tr-17603-31-12-2021>